International Journal of Innovative
Computing, Information and Control
Volume **8**, Number **9**, September **2012**

 ISSN 1349-4198
pp. **6049–6066**

A BEE COLONY OPTIMIZATION BASED-FUZZY LOGIC-PID CONTROL DESIGN OF ELECTROLYZER FOR MICROGRID STABILIZATION

Theerawut Chaiyatham and Issarachai Ngamroo

School of Electrical Engineering
Faculty of Engineering
King Mongkut's Institute of Technology Ladkrabang
Chalongkrung Road, Bangkok 10520, Thailand
ngamroo@gmail.com

Received May 2011; revised September 2011

Abstract. *This paper proposes the optimal fuzzy logic based-proportional-integral-derivative (FLPID) controller design of the electrolyzer (EZ) by a bee colony optimization (BCO) for microgrid (MG) stabilization. The study MG system consists of wind power (WP), photovoltaic (PV), fuel cell (FC) equipped with EZ, diesel generator, and load. The intermittent power generations from WP and PV cause the severe power fluctuation in the MG. To alleviate power fluctuation, the EZ which is normally used to produce the hydrogen input for FC, can be applied. By control of active and reactive powers absorbed by EZ, the power fluctuation can be stabilized. The structure of active and reactive power controllers of EZ is the FLPID which consists of scale factors (SCs), membership functions (MFs), and control rules (CRs). Without trial and error, SCs, MFs, and CRs of the FLPID controller are automatically optimized by a BCO. Simulation study confirms that the proposed EZ with an optimal FLPID controller is much superior to the EZ with a conventional FLPID controller or an optimal PID controller in terms of stabilizing effect and robustness against various loading conditions and severe disturbances.*
Keywords: Electrolyzer, Microgrid, Fuzzy PID control, Bee colony optimization

1. **Introduction.** Nowadays, the microgrid (MG) is expected as the smart electrical power management for rural and isolated areas that cannot access to the main power grid due to the restriction of installation costs of transmission lines, right of way difficulties, social, and environmental impacts [1]. The MG is the cluster of the distributed generation with renewable energy sources and/or conventional generating units and loads [2]. At present, there are many MG projects around the world such as Kythnos Island MG in Greece [2], Aichi, Kyotango and Hachinohe MG projects in Japan [3], and the Consortium for Electric Reliability Technology Solutions (CERTS) project in the United States [4], etc.

Generally, renewable energy sources such as wind power (WP), photovoltaic (PV), fuel cell (FC) with electrolyzer (EZ), are usually installed in the MG, since these sources are inexhaustible, environmental friendly, clean, and no CO_2 emission [5]. These renewable energy sources are often operated with the conventional electricity generations such as diesel generator (DG), and gas turbine. Nevertheless, the solar and wind energy are intermittent in nature. The power generation from WP and PV is variable [6]. This causes the power unbalance in generation and load [7], and results in the severe power fluctuation in the MG [8-10]. To suppress the power fluctuation, several methods have been proposed in previous works [11-14]. Recent advancement in the EZ equipped with an FC has opened up options for using hydrogen as an energy storage. In addition to a

hydrogen production for an FC input, the EZ can be used as the controllable load [15,16]. Moreover, the power absorbed by EZ can be rapidly controlled to compensate for power fluctuation in the MG [17].

In recent years, many works have been conducted on control system stabilization. However, all those control design methods require the exact mathematical model of the control systems which may not be available in practice. On the other hand, a fuzzy logic control has been successfully employed for solving many nonlinear control problems. Without exact mathematical model of the control system, the fuzzy controller can be designed. In [18], the fuzzy decentralized state feedback and observer-based decentralized output feedback controllers for a class of continuous nonlinear interconnected systems with time-delay and the modelling error have been applied. In [19], the sliding mode controller with fuzzy logic has been used for the heading control of the submersible vehicle. In [20], the method of fuzzy control systems for trailers driven by multiple motors in side slipways to haul out ships has been presented. In [21], the fuzzy logic controller with interval-valued inference mechanism has been applied for the control of distributed parameter system. Besides, the fuzzy logic based-proportional-integral-derivative (FLPID) controller has been proposed in [22]. In these works, nevertheless, the selection of scale factors (SF), membership functions (MF), and control rules (CR) of the FLPID controller is still the inevitable problem and depends on the designer's experience.

To overcome this problem, this paper proposes the new optimal FLPID controller design of EZ for alleviation of power fluctuation in the MG with hybrid power generations such as WP, PV, FC with EZ, and DG. The intermittent power generations from WP and PV result in severe power fluctuation in the MG. With the fast response of EZ, the power absorbed by an EZ can be rapidly controlled to compensate for power fluctuation. To achieve the optimal SF, MF, and CR of the FLPID, this paper applies a bee colony optimization (BCO) [23] to automatically tune these parameters of the FLPID. Simulation study is carried out in the nonlinear MG model. The proposed EZ with an optimal FLPID controller not only shows superior stabilizing effect than the EZ with a conventional FLPID or optimal PID controller, but also provides high robustness under various operating conditions and large disturbances.

2. **Study System and Modeling.** A single line diagram of a stand-alone MG [24] is depicted in Figure 1. It consists of 20 MVA DG, 4 MW WP, 800 kW PV, 3 MW EZ, 2 MW FC and $10+j2$ MVA load. The system MVA base is set at 20 MVA. System parameters are given in Table 1. The DG is represented by a 3rd-order synchronous generator model [25]. It is equipped with a simplified 1st-order model of exciter and governor [25]. Since the response of the converters equipped with WP and PV is very fast, these converters have not been included in the WP and PV models for the sake of simplicity. Here, the WP and PV are represented by the random active power source model [17]. The intermittent power generations from WP and PV cause power fluctuation in the MG.

Figure 2(a) depicts the simplified model of the study MG. The negative sign implies the absorbed power by EZ from the system while the positive sign of other power sources means the power supply to the system. The difference between supplied and absorbed powers is shown by active power deviation (ΔP) and reactive power deviation (ΔQ) which are controlled by EZ to be minimum.

As shown in Figure 1, it is assumed that the converter used for an EZ is the voltage source converter type. Normally, the role of the converter is used to absorb AC power from the system and convert to DC power for a hydrogen production as an FC input. In this work, the converter is also applied to control the active and reactive powers absorbed from the system by the FLPID controller with the objective of alleviation of power fluctuation

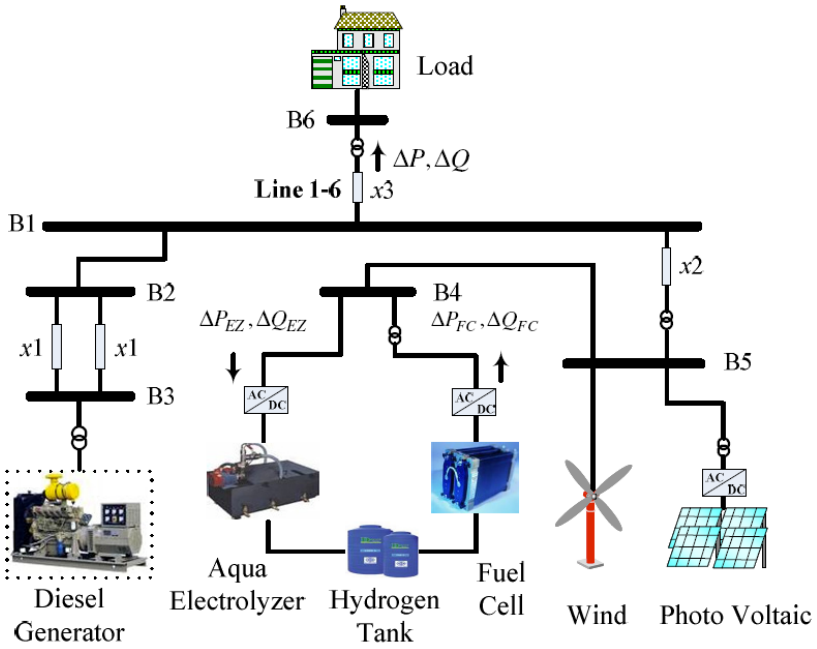

FIGURE 1. A stand-alone microgrid

TABLE 1. System parameters

Devices	Parameters	values
Diesel Generator	Armature resistance R_a	0.0036 pu
	d-axis synchronous reactance X_d	1.56 pu
	q-axis synchronous reactance X_q	1.06 pu
	d-axis transient reactance X'_d	0.296 pu
	d-axis open circuit transient time constant T'_{d0}	1.01 s
	Inertia coefficient H	0.8 s
Transmission line	Reactance $x1$	0.4 pu
	Reactance $x2$	0.2 pu
	Reactance $x3$	0.5 pu

in the system. Based on the ability of independent and simultaneous control of active and reactive powers by the converter, the active and reactive power controllers of EZ can be shown separately in Figure 2(b). As the power source model, the converter dynamic can be represented by the 1st-order transfer function [26-28]. The converter gain K_E and time constant T_E are set at 5.0 and 0.2, respectively [26]. The active and reactive power deviations absorbed by EZ (ΔP_{EZ} and ΔQ_{EZ}) are controlled by the FLPID of P and Q controllers, respectively. The active and reactive power deviations in the line 1-6 (ΔP and ΔQ) are used as the input signals of P and Q controllers, respectively.

Figure 2(c) shows the hydrogen production model [26]. The block diagram of a power to hydrogen transfer shows the rate of a hydrogen production by the absorbed power from an EZ (P_{EZ}) as well as the rate of a hydrogen usage for a power production by an FC (P_{FC}). Here, the EZ absorbs the active and reactive powers from the system in order to produce the hydrogen with the rate of 0.029 l/kWh. The produced hydrogen is stored in the 500 litre hydrogen tank. The FC uses the hydrogen in the tank as the input fuel and converts to the active and reactive power outputs with the rate of 0.061 l/kWh.

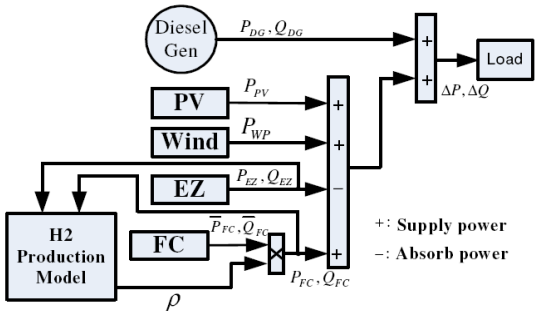

(a) Simplified diagram

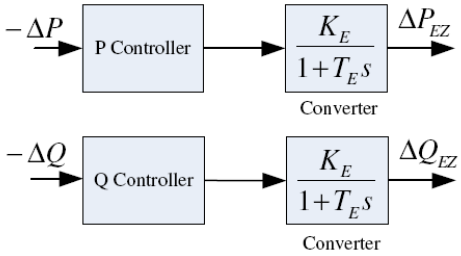

(b) EZ model with P and Q controllers

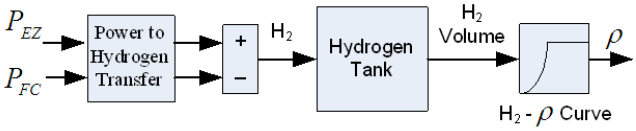

(c) Hydrogen production model

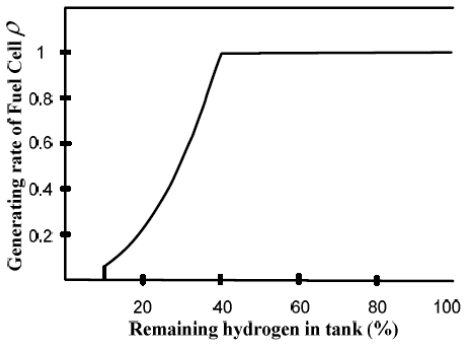

(d) Relation of the remaining hydrogen in the tank and the generating rate of FC

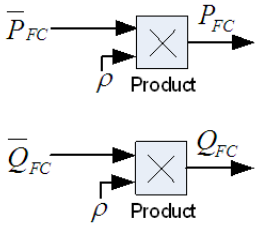

(e) FC model

FIGURE 2. MG modelling

The difference between a hydrogen production by an EZ and a hydrogen usage by an FC becomes the remaining hydrogen in the tank.

In this study, the operating method of FC generators has two limitations. These limitations are very important in reduction of a start-up and a shutdown of FC generators since a voltage of FC drops due to its start-up and shutdown operations [26]. These two limitations are given as follows.

i If the remaining amount of the hydrogen drops below 10% of a hydrogen tank capacity, the FC stops. The FC continues to stop until the capacity of the hydrogen reaches 50%.

ii The generating rate of the FC (ρ) varies with the remaining fuel in the hydrogen tank. The relation between the remaining fuel in hydrogen tank and the generating rate is shown in Figure 2(d) [26].

For the FC model, it is represented by the constant power source model as shown in Figure 2(e). The active and reactive power output commands ($\bar{P}_{FC}$ and $\bar{Q}_{FC}$) of FC are kept constant at 0.05 pu and 0 pu, respectively. From the limitation (ii), the actual generating power of FC (P_{FC} and Q_{FC}) is represented by the product of the generating rate and the output command of FC as

$$\begin{aligned} P_{FC} &= \rho \overline{P}_{FC} \\ Q_{FC} &= \rho \overline{Q}_{FC} \end{aligned} \tag{1}$$

3. **Proposed Optimized FLPID Controller.** The main idea of fuzzy logic system was introduced by Zadeh in 1965 [29], and first applied to control theory in 1974 by Mamdani [30]. Based on these works, the fuzzy controllers have successfully been employed for various applications [31-33]. One of most popular type of fuzzy logic control is the FLPID controller as shown in Figure 3, because the FLPID is able to eliminate steady state error and good performance during the transient state [34].

Figure 3 shows the proposed FLPID for P-Q controllers of EZ. The input signal e is the active power deviation in the line 1-6 for P controller or reactive power deviation in the line 1-6 for Q controller. The output signal of FLPID controller is given by

$$u = \alpha y + \beta \int y \, dt \tag{2}$$

It has been shown in [22] that for the product – sum crisp type fuzzy controller, the relation between the input and the output variables of the fuzzy logic controller can be given as

$$y = A + BE + DE' \tag{3}$$

where $E = K_e e$ and $E' = K_d e'$. Therefore, from (2) and (3), the controller output is obtained as

$$u = \alpha A + \beta A t + \alpha K_e B e + \beta K_d D e + \beta K_e B \int e \, dt + \alpha K_d D e^{\bullet} \tag{4}$$

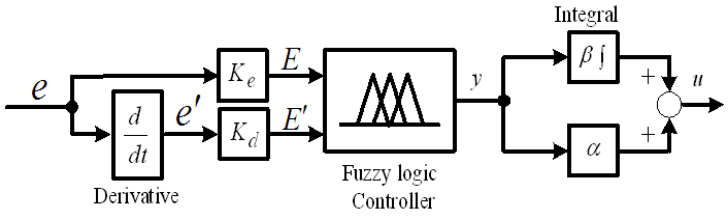

FIGURE 3. Block diagram of FLPID controller

Thus, the equivalent control components of the FLPID type are obtained as follows:

- Proportional gain: $\alpha K_e P + \beta K_d D$
- Integral gain: $\beta K_e P$
- Derivative gain: $\alpha K_d D$

In case of the design of FLPID controller, there are four tuning parameters of SFs i.e., K_e, K_d, β and α. Besides, there are many tuning parameters of MFs and CRs. Here, consider two shapes of MF, i.e., triangular and trapezoidal memberships which are shown in Figure 4. A triangular membership is defined by three parameters, i.e., left base (L), centre (C), and right base (R). For a trapezoidal membership, it is defined by four parameters, i.e., left base (L), centre 1 (C_1), centre 2 (C_2), and right base (R). Each MF is composed of two trapezoidal memberships and five triangular memberships. Accordingly, it has 23 $(4+3+3+3+3+3+4=23)$ tuning parameters. The fuzzy logic controller has two-inputs and one-output. Therefore, there are 69 $(3 \times 23 = 69)$ tuning parameters.

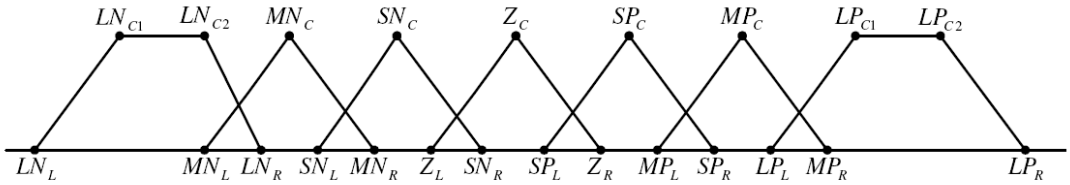

LN: large negative; MN: medium negative; SN: small negative;
Z: zero; SP: small positive; MP: medium positive;
LP: large positive.

FIGURE 4. The shape of membership functions

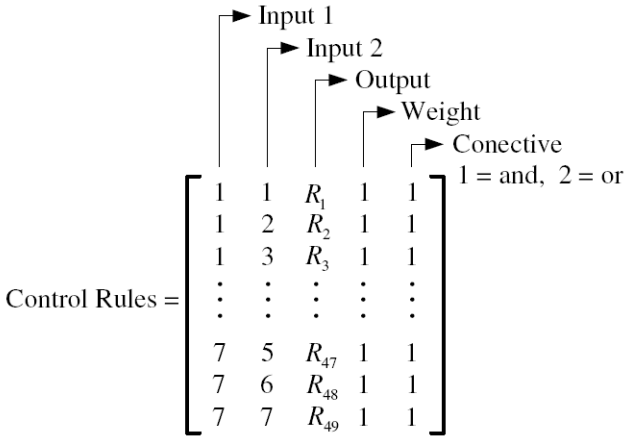

FIGURE 5. Structure of control rules for fuzzy logic controller

The CRs for two-inputs and one-output fuzzy logic controller is represented by n rows and 5 columns matrix as shown in Figure 5. When this idea is applied to the fuzzy logic toolbox, n is the total number of relationships between all possible input pairs (for 7 MFs, $n = 7^2 = 49$). The third column in the control rule table is the linguistic variable outputs. Generally, it is represented by a numeric symbol. The universe of discourse in this study contains seven memberships. Consequently, the control rules are represented by seven numbers (1to 7), 1: LN, 2: MN, 3: SN, 4: Z, 5: SP, 6: MP, and 7: LP. Note

that there are 49 tuning parameters. Therefore, the total parameters for two-inputs and one-output FLPID controller are 122 $(4 + 69 + 49 = 122)$.

In the FLPID controller design, the important procedure is how to determine the SFs, MFs, and CRs. In general, they are determined by the trial and error and designer's experiences. To overcome this problem, this study applies a BCO algorithm to automatically determine the SFs, MFs and CRs.

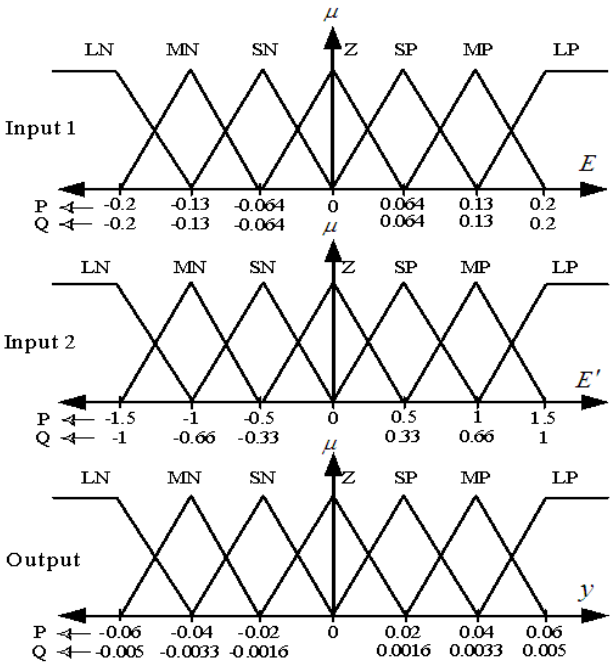

(a) Membership functions

Input 1 \ *Input* 2	LN	MN	SN	Z	SP	MP	LP
LN	LP	LP	LP	MP	MP	SP	Z
MN	LP	MP	MP	MP	SP	Z	SN
SN	LP	MP	SP	SP	Z	SN	MN
Z	MP	MP	SP	Z	SN	MN	MN
SP	MP	SP	Z	SN	SN	MN	LN
MP	SP	Z	SN	MN	MN	MN	LN
LP	Z	SN	MN	MN	LN	LN	LN

(b) Control rules

FIGURE 6. P and Q controllers design of EZ with a conventional FLPID

Figure 6 shows the MFs and CRs before optimization of the conventional FLPID. Three MFs with two-input and one-output of the FLPID are depicted in Figure 6(a). For the case of two-input and one-output, the CRs can be depicted graphically in Figure 6(b), where every cell shows the output MF of a CR with two input MFs. The CRs are built from the statement: if input 1 and input 2 then output 1. For example, consider the third row and forth column in Figure 6(b), that means: if E is SN and E' is Z, then u is SP. The FLPID controller which uses the MFs and the CRs as shown in Figure 6, is

referred to as the "Conventional FLPID controller". Note that only the SFs are tuned for conventional FLPID. On the other hand, for the proposed controller which is referred to as the "Optimal FLPID controller", the SFs, MFs, and CRs are automatically tuned.

The optimization problem for optimal PID, conventional FLPID and optimal FLPID controllers is formulated based on the minimization of the integral absolute error (IAE) of the line power deviations as,

$$\text{Minimize } IAE = \int_0^t \left(|\Delta P(t)| + |\Delta Q(t)|\right) dt \tag{5}$$

This optimization problem is solved by BCO.

4. **Bee Colony Optimization.** The BCO algorithm mimics the food foraging behaviour of swarms of honey bees [23]. Honey bees use several mechanisms like waggle dance to optimally locate food sources and search new ones. This makes them a good candidate for developing new intelligent search algorithms. It is a very simple, robust and population based stochastic optimization algorithm. The procedure of the BCO algorithm for tuning FLPID parameters as shown in Figure 7 can be described as below:

Step 1: Generate randomly the initial populations of n scout bees for the parameters of SF, MF, and CR. These initial populations must be feasible candidate solutions that satisfy the constraints. Set $NC = 0$.
Step 2: Represent the value of SF, MF, and CR from each population.
Step 3: Evaluate the fitness value of the initial populations by (5).
Step 4: Select m best sites for neighborhood search. Separated the m best sites to two groups, the first group has e best sites and another group has $m - e$ best sites.
Step 5: Determine the size of neighborhood search of each best size (patch size, ngh).
Step 6: Recruit bees of ne employed bees for selected sites (more bees for the best e sites).
Step 7: Represent the value of SF, MF, and CR from each employed bee.
Step 8: Select the fittest bees from each patch.
Step 9: Check the stopping criterion. If satisfied, terminate the search, else $NC = NC + 1$.
Step 10: Assign the $n - m$ remaining bees to random search. Go to Step 2.

where ns is number of scout bee, NC is number of iteration, m is number of sites selected for neighborhood search, e is number of best "elite" sites out of m selected sites and ne is number of employed bee.

The motivation of the practical use of the theoretic results obtained from the proposed method is the automatic optimization of SFs, MFs, and CRs for the FLPID controller by BCO. Without trial and error and designer's experience, the optimal FLPID controller can be automatically tuned. In addition, the proposed method can be practically applied in industrial systems such as a fuzzy control design in a tunnel lighting system [35], a fuzzy control design in a wire transport system of wire electrical discharge machining machine [36], a fuzzy control design in a fuel-cell hybrid tramway [37], and a fuzzy control design for a gas engine driven heat pump [38] etc. The application of the proposed method to these practical systems not only considerably simplifies the fuzzy control design, but also significantly enhances the control effect.

However, the deficiency of the proposed technique is that the trained parameters obtained from some case studies cannot guarantee the control effect of the designed FLPID

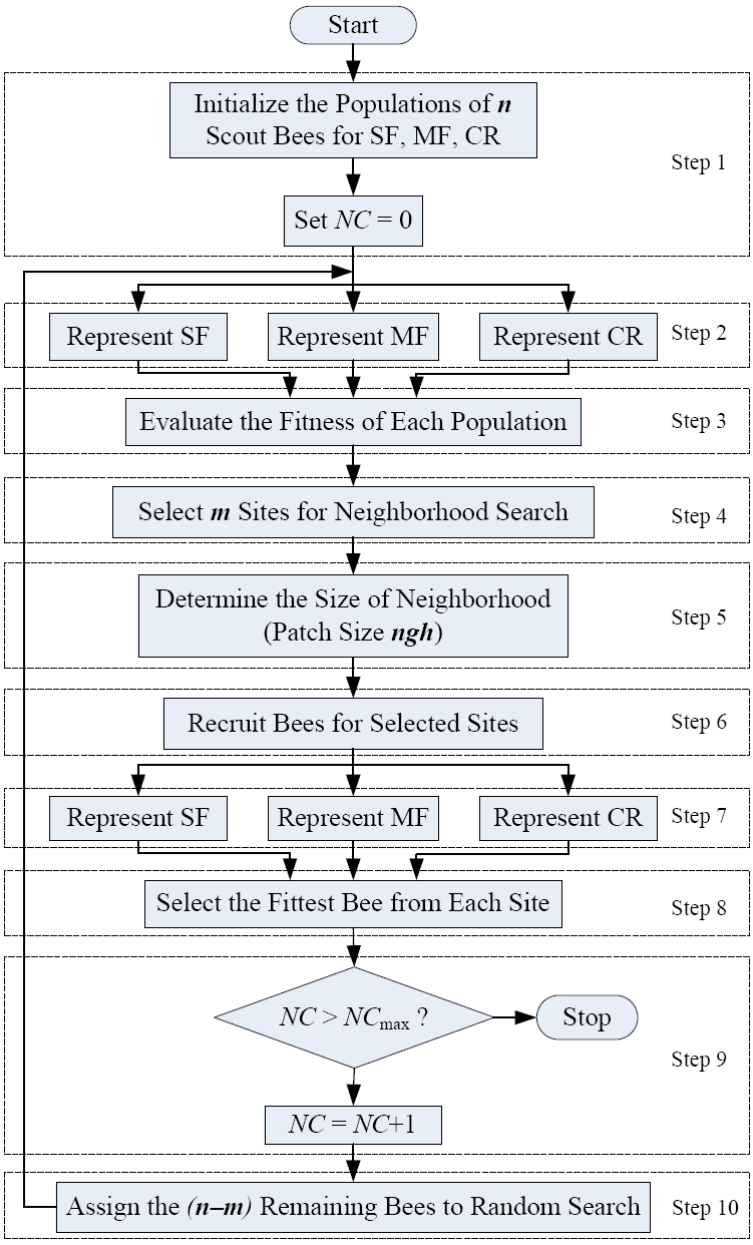

FIGURE 7. Procedure of BCO algorithm for tuning FLPID parameters

controller. The control effect of FLPID may be deteriorated when the control signal input differs from the trained data. To overcome this problem, the parameters of FLPID controller should be designed by several trained data of many case studies.

5. **Simulation Study.** To show the superior effect of the EZ with an optimal FLPID controller, the following controllers are designed individually for comparison studies.

1) The EZ with an optimal PID controller.
2) The EZ with a conventional FLPID controller.
3) The EZ with an optimal FLPID controller.

In the optimization of EZ with each controller, it is supposed that the WP and PV with 180 s in Figure 8 are applied to the MG. Note that the trained parameters obtained by 180 s of the simulation period (short-term) can be applied to the long-term optimization.

Although the optimization with long-term provides better result than that with short-term, it takes longer time in the optimization. If the data of short-term and long-term are not much different, the short-term data is preferable. Here, the constant parameters in BCO are set as follows: $ns = 100$, $ne = 10$, $m = 10$, $e = 4$, $ngh = 30\%$ and $NC = 100$.

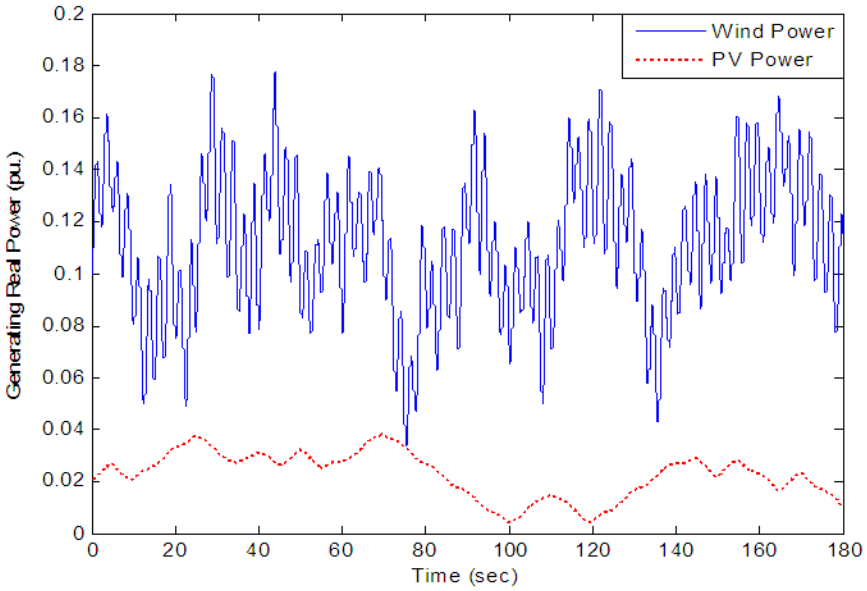

FIGURE 8. WP and PV outputs

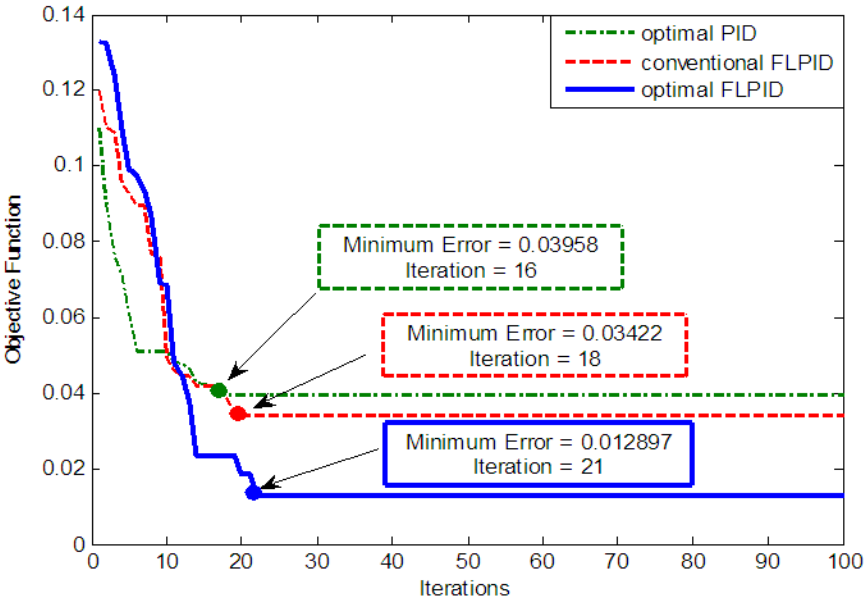

FIGURE 9. Convergence curves

As a result, the convergence curves of the EZ with an optimal PID, the EZ with a conventional FLPID, and the EZ with an optimal FLPID are shown in Figure 9. They start at the different initial values and gradually decrease to the minimum values. Besides, the MF and CR of P and Q controllers of EZ are delineated in Figures 10 and 11,

respectively. For example of the MF before and after optimizations in Figure 10(a), the left base value, the centre value, and the right base value of the optimized membership Z have been moved from −0.064, 0, 0.064 to −0.035, 0, 0.046, respectively. For example of the CR before and after optimizations, the encircled rule "LP" before optimization in Figure 6(b) has been changed to the encircled "MP" after optimization in Figures 10(b) and 11(b). The optimized parameters of P and Q controllers of EZ can be automatically achieved as in Tables 2 and 3, respectively. Besides, the PID control parameters of EZ are obtained by the same proposed method as shown in Table 4.

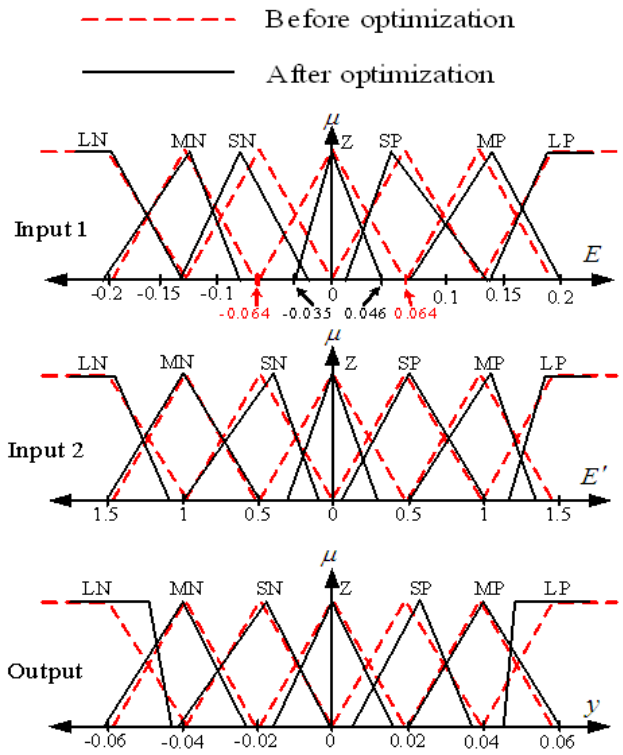

(a) Membership functions

Input 1 \ Input 2	LN	MN	SN	Z	SP	MP	LP
LN	LP	LP	MP	MP	SP	SP	Z
MN	(MP)	MP	MP	SP	SP	Z	Z
SN	MP	SP	SP	SP	Z	SN	SN
Z	MP	SP	Z	Z	SN	SN	MN
SP	MP	SP	Z	SN	SN	MN	MN
MP	SP	Z	SN	SN	MN	MN	MN
LP	Z	SN	SN	SN	MN	MN	LN

(b) Control rules

FIGURE 10. P controller design of the proposed EZ with an optimal FLPID

Nonlinear simulations are carried out for four case studies.
Case 1: The MG is operated under power generations from WP and PV in Figure 8.

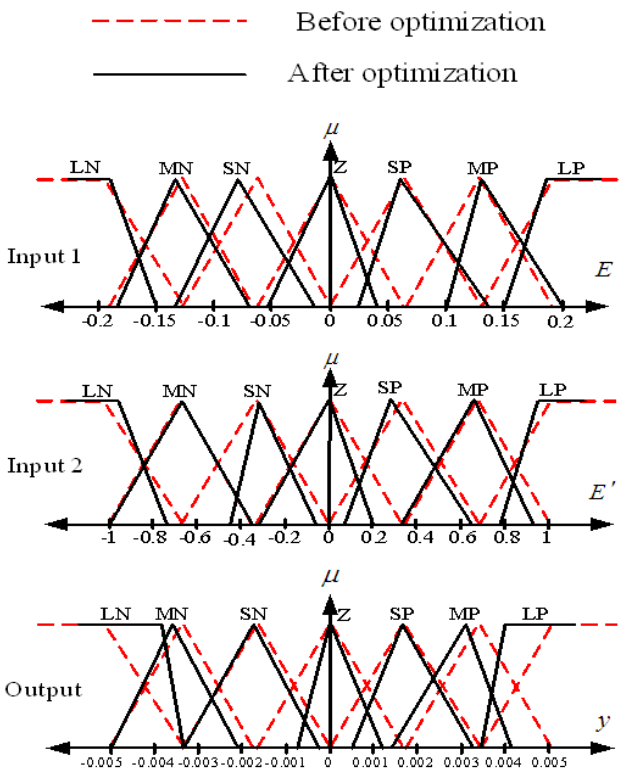

(a) Membership functions

Input 1 \ Input 2	LN	MN	SN	Z	SP	MP	LP
LN	MP	MP	MP	MP	SP	SP	Z
MN	MP	MP	SP	SP	SP	Z	SN
SN	SP	SP	SP	Z	Z	SN	SN
Z	MP	SP	SP	Z	Z	SN	SN
SP	SP	SP	Z	Z	SN	SN	MN
MP	SP	Z	SN	SN	SN	MN	MN
LP	Z	SN	SN	SN	SN	MN	MN

(b) Control rules

FIGURE 11. Q controller design of the proposed EZ with an optimal FLPID

TABLE 2. Control parameters of P controller

Controller	K_e	K_d	β	α	MF	CR
Conventional FLPID	0.7294	0.518	0.4623	0.3761	Figure 6(a)	Figure 6(b)
Optimal FLPID	0.7783	0.881	0.6821	0.2275	Figure 10(a)	Figure 10(b)

TABLE 3. Control parameters of Q controller

Controller	K_e	K_d	β	α	MF	CR
Conventional FLPID	1.047	0.625	1.1328	0.1196	Figure 6(a)	Figure 6(b)
Optimal FLPID	0.983	0.869	1.0616	0.1504	Figure 11(a)	Figure 11(b)

TABLE 4. PID control parameters of P and Q controllers

Controller	K_P	K_I	K_D
P Controller	0.357	0.056	0.052
Q Controller	0.195	0.042	0.049

Simulation results for 2,000 s are depicted in Figure 12. As shown in Figures 12(a) and 12(b), without EZ controller, the active and reactive power flows in the lines 1-6 severely fluctuate. On the other hand, the EZs with an optimal PID, conventional FLPID and optimal PID are able to alleviate the power fluctuation effectively. Nevertheless, the EZ with an optimal FLPID provides better damping effect than EZ with conventional FLPID or optimal PID. The absorbed active and reactive powers of EZ are demonstrated in Figures 12(c) and 12(d), respectively. The power absorbed by the EZ with an optimal FLPID is higher than that of the EZ with conventional FLPID or optimal PID. Accordingly, the active and reactive power fluctuations in the line 1-6 in case of the EZ with an optimal FLPID are lower than those of the EZ with conventional FLPID or optimal PID.

Case 2: Assume that the power generations from WP and PV in Figure 8 decrease by 50%. At $t = 0.5$ s, the active power of load suddenly increases from 0.6 pu to 0.8 pu.

Simulation results of active and reactive power deviations in the line 1-6 are shown in Figures 13(a) and 13(b), respectively. In comparison to the EZ with a conventional FLPID or optimal PID, the EZ with an optimal FLPID shows better stabilizing effect.

Case 3: Assume that the power generations from WP and PV in Figure 8 decrease by 50% while the random step load occurs as shown in Figure 14(a).

Simulation results of active and reactive power fluctuations in the line 1-6 are shown in Figures 14(b) and 14(c), respectively. The EZ with a conventional FLPID is very sensitive to the disturbances. The power oscillations are higher and very severe. On the contrary, the proposed EZ with an optimal FLPID is robustly capable of damping the power oscillations.

Case 4: Assume that the power generations from WP and PV in Figure 8 decrease by 35%. The three phase fault to ground occurs at $t = 0.5$ s for 70 ms and is cleared naturally.

Simulation results of active and reactive power fluctuations in the line 1-6 are depicted in Figure 15(a) and 15(b), respectively. It can be observed that the stabilizing effect of the EZ with a conventional FLPID is considerably deteriorated by the three-phase fault. The damping of power oscillation is very poor. On the other hand, the proposed EZ with an optimal FLPID can tolerate this severe disturbance. It is able to damp out power oscillations robustly.

6. **Conclusion.** The BCO-based optimal FLPID control design of EZ for stabilization of power fluctuation in a stand-alone MG has been presented in this paper. The active and reactive power controllers of EZ are optimized by the proposed design.

The unique features and the main advantages which make the proposed BCO based FLPID superior over other fuzzy control approaches can be summarized as follows.

1) Without trial and error, all adjusting parameters of the FLPID controller, i.e. SCs, MFs, and CRs are automatically and simultaneously optimized by a BCO. As a result, the optimal FLPID controller can be guaranteed.

2) The designed FLPID controller is very effective and robust because it can deal with various disturbances and system uncertainties such as various loading conditions and

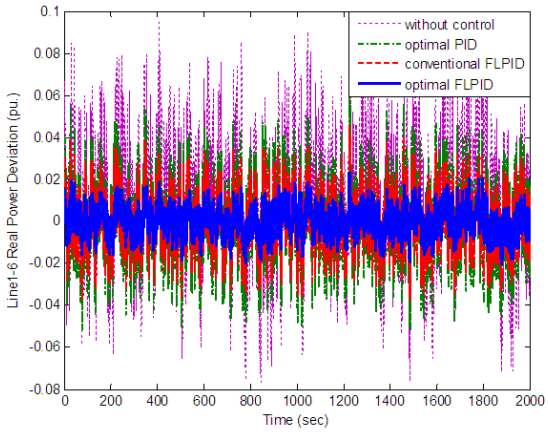

(a) Active power deviation in line 1-6

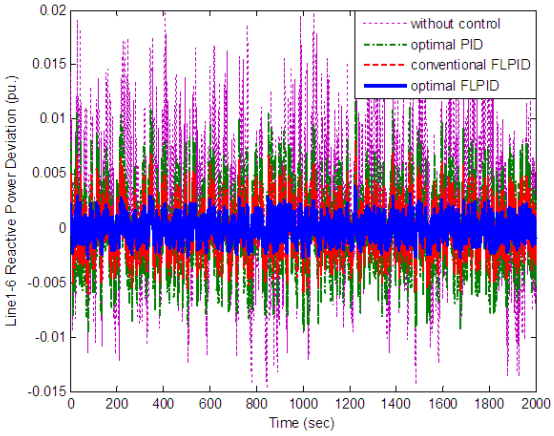

(b) Reactive power deviation in line 1-6

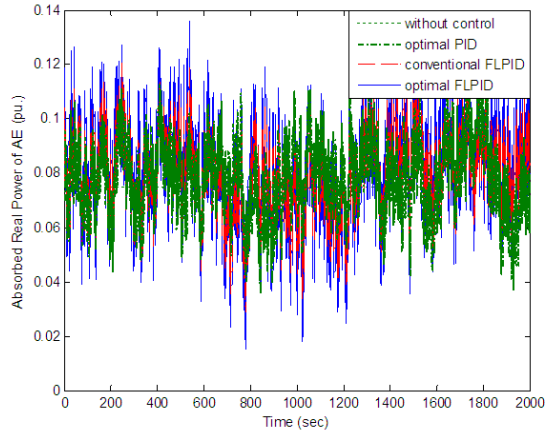

(c) Absorbed real power of EZ

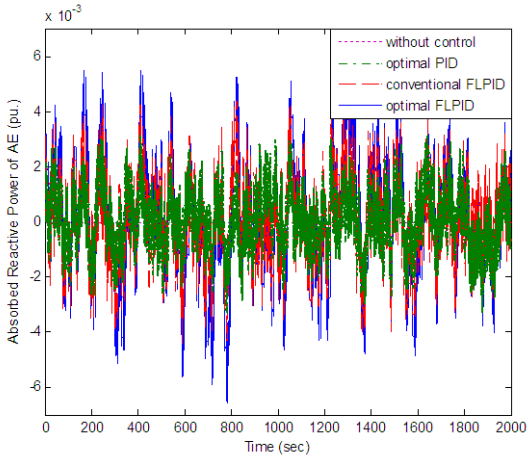

(d) Absorbed reactive power of EZ

FIGURE 12. Simulation results in case 1

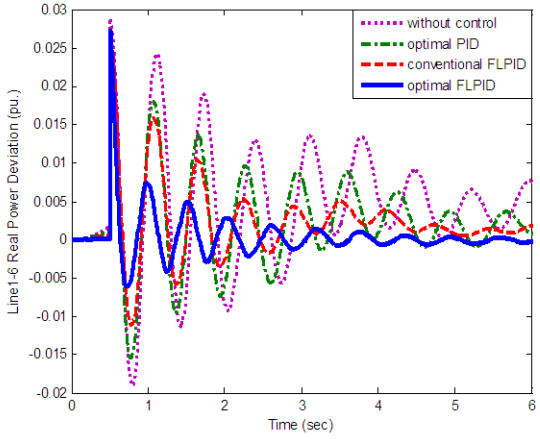

(a) Active power deviation in line 1-6

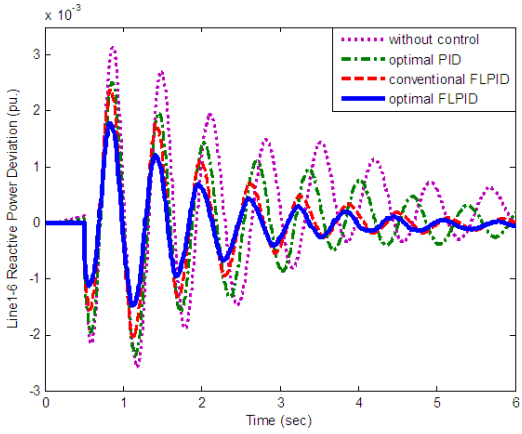

(b) Reactive power deviation in line 1-6

FIGURE 13. Simulation results in case 2

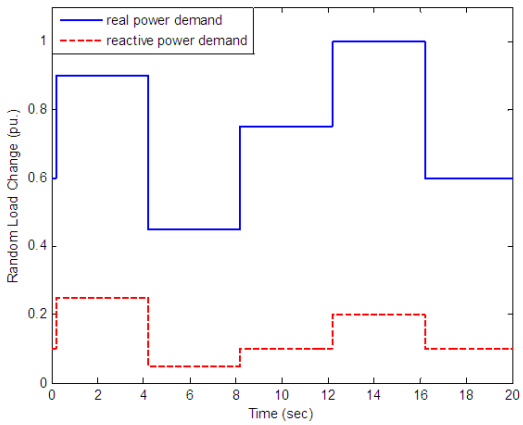

(a) Random load changes

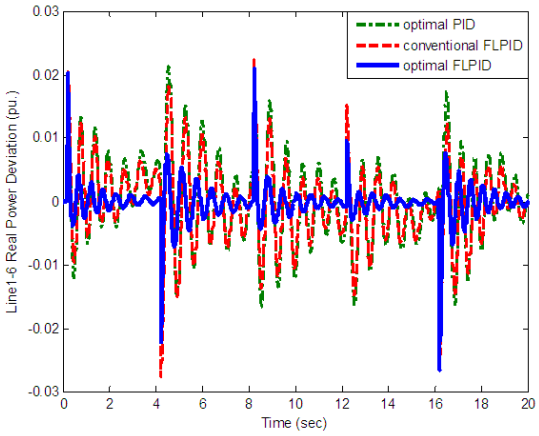

(b) Active power deviation in line 1-6

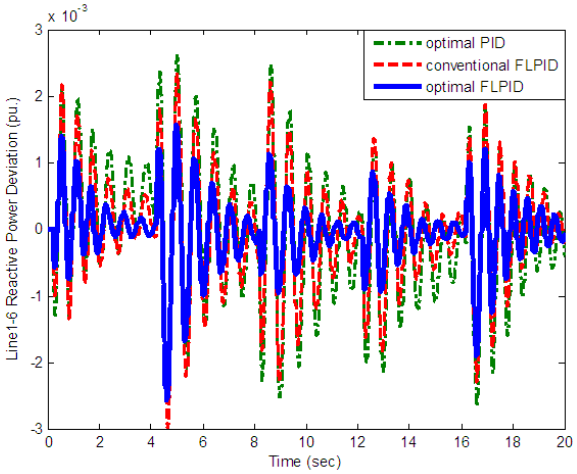

(c) Reactive power deviation in line 1-6

FIGURE 14. Simulation results in case 3

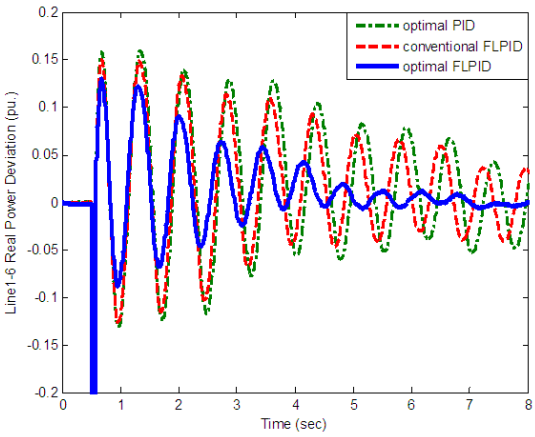

(a) Active power deviation in line 1-6

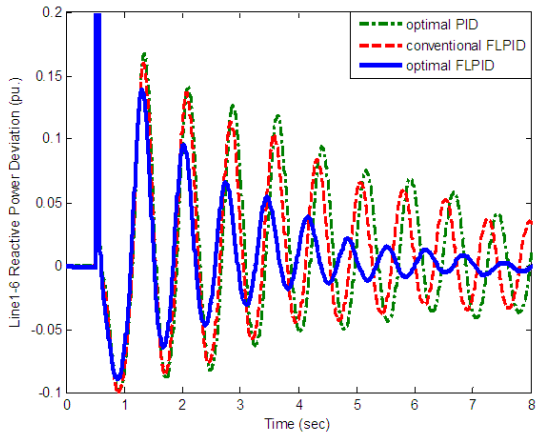

(b) Reactive power deviation in line 1-6

FIGURE 15. Simulation results in case 4

severe faults etc. The superior effectiveness and robustness of the proposed FLPID controller in comparison with the conventional FLPID controller and optimal PID controller have been confirmed by various case studies.

The convincing and practical examples of the proposed techniques to demonstrate the advantages and effectiveness are given as follows:

1) Load frequency control of hydro-electrical power plants [39].
2) Intelligent control of elevator systems [40].
3) Energy saving for multi-unit room air-conditioners [41].
4) The control of weld line positions in injection-molded part [42].

Acknowledgment. This work is supported by the King Mongkut's Institute of Technology Ladkrabang Research Fund. The authors also gratefully acknowledge the helpful comments and suggestions of the reviewers, which have improved the presentation.

REFERENCES

[1] J. Park, W. Liang, J. Choi, A. A. El-Keib and J. Watada, Probabilistic production cost credit evaluation of wind turbine generators, *International Journal of Innovative Computing, Information and Control*, vol.5, no.11(A), pp.3637-3646, 2009.

[2] N. Hatziargyriou, H. Asano, R. Iravani and C. Marnay, Microgrids, *IEEE Power and Energy Magazine*, vol.5, no.4, pp.78-94, 2007.

[3] S. Morozumi, Micro-grid demonstration projects in Japan, *Proc. of IEEE Power Conversion Conference*, vol.6, pp.35-42, 2007.

[4] B. Kroposki, R. Lasseter, T. Ise, S. Morozumi, S. Papathanassiou and N. Hatziargyriou, Making microgrids work, *IEEE Power and Energy Magazine*, vol.6, no.3, pp.40-53, 2008.

[5] M. Calderón, A. J. Calderón, A. Ramiro and J. F. González, Weather data and energy balance of a hybrid photovoltaic-wind system with hydrogen storage, *International Journal of Hydrogen Energy*, vol.35, no.15, pp.7706-7715, 2010.

[6] G. Giannakoudis, A. I. Papadopoulos, P. Seferlis and S. Voutetakis, Optimum design and operation under uncertainty of power system using renewable energy sources and hydrogen storage, *International Journal of Hydrogen Energy*, vol.35, no.3, pp.872-891, 2010.

[7] S. Obara and A. G. El-Sayed, Compound microgrid installation operation planning of a PEFC and photovoltaics with prediction of electricity production using GA and numerical weather information, *International Journal of Hydrogen Energy*, vol.34, no.19, pp.8213-8222, 2009.

[8] J. L. Márquez, M. G. Molina and J. M. Pacas, Dynamic modelling, simulation and control design of an advanced micro-hydro power plant for distributed generation applications, *International Journal of Hydrogen Energy*, vol.35, no.11, pp.5772-5777, 2010.

[9] M. Little, M. Thomson and I. Infield, Electrical integration of renewable energy into stand-alone power supplies incorporating hydrogen storage, *International Journal of Hydrogen Energy*, vol.32, no.10-11, pp.1582-1588, 2007.

[10] F. Gutiérrez-Martín, D. Confente and I. Guerra, Management of variable electricity loads in wind – Hydrogen systems: The case of a Spanish wind farm, *International Journal of Hydrogen Energy*, vol.35, no.14, pp.7329-7336, 2010.

[11] M. Uzunoglu and O. C. Onar, Static var compensator reactive power management for SOFC power plants, *International Journal of Hydrogen Energy*, vol.33, no.9, pp.2367-2378. 2008.

[12] M. Calderón, A. J. Calderón, A. Ramiro and J. F. González, Automatic management of energy flows of a stand-alone renewable energy supply with hydrogen support, *International Journal of Hydrogen Energy*, vol.35, no.6, pp.2226-2235, 2010.

[13] D. Ramirez, L. F. Beites, F. Blazquez and J. C. Ballesteros, Distributed generation system with PEM fuel cell for electrical power quality improvement, *International Journal of Hydrogen Energy*, vol.33, no.16, pp.4433-4443, 2008.

[14] M. G. Molina and P. E. Mercado, Stabilization and control of tie-line power flow of microgrid including wind generation by distributed energy storage, *International Journal of Hydrogen Energy*, vol.35, no.11, pp.5827-5833, 2010.

[15] E. Troncoso and M. Newborough, Electrolysers as a load management mechanism for power systems with wind power and zero carbon thermal power plant, *Applied Energy*, vol.87, no.1, pp.1-15, 2010.

[16] E. Troncoso and M. Newborough, Implementation and control of electrolysers to achieve high penetrations of renewable power, *International Journal of Hydrogen Energy*, vol.32, no.13, pp.2253-2268, 2007.
[17] S. Vachirasricirikul, I. Ngamroo and S. Kaitwanidvilai, Application of electrolyzer system to enhance frequency stabilization effect of microturbine in a microgrid system, *International Journal of Hydrogen Energy*, vol.34, no.17, pp.7131-7142, 2009.
[18] S. Tong, S. Tong and Q. Zhang, Robust stabilization of nonlinear time-delay interconnected systems via decentralized fuzzy control, *International Journal of Innovative Computing, Information and Control*, vol.4, no.7, pp.1567-1582, 2008.
[19] X. Song, J.-W. Ye and L.-M. Wu, Application of the integral sliding mode controller with fuzzy logic to submersible vehicle, *International Journal of Innovative Computing, Information and Control*, vol.3, no.4, pp.897-906, 2007.
[20] N. Aung, E. Cooper, Y. Hoshino and K. Kamei, A proposal of fuzzy control systems for trailers driven by multiple motors in side slipways to haul out ships, *International Journal of Innovative Computing, Information and Control*, vol.3, no.4, pp.799-812, 2007.
[21] S. Li and X. Zhang, Fuzzy logic controller with interval-valued inference for distributed parameter system, *International Journal of Innovative Computing, Information and Control*, vol.2, no.6, pp.1197-1206, 2006.
[22] Z. Q. Wu and M. Mizumoto, PID type fuzzy controller and parameter adaptive method, *Fuzzy Sets and Systems*, vol.78, no.1, pp.23-36, 1996.
[23] D. Karaboga, An idea based on honey bee swarm for numerical optimization, *Technical Report-Tr06t*, Erciyes Univ., Turkey, 2005.
[24] T. Senjyu, D. Hayashi, R. Sakamoto, N. Urasaki and T. Funabashi, Generating power levelling of renewable energy for small power system in isolated island, *IEEJ Trans. on Power and Energy*, vol.25, no.12, pp.1209-15, 2005.
[25] P. Kundur, *Power System Stability and Control*, McGraw Hill, 1994.
[26] T. Senjyu, T. Nakaji, K. Uezato and T. Funabashi, A hybrid power system using alternative energy facilities in isolated island, *IEEE Trans. on Energy Conversion*, vol.20, no.2, pp.406-414, 2005.
[27] T. Ise, Y. Murakami and K. Tsuji, Simultaneous active and reactive power control of superconducting magnet energy storage using GTO converter, *IEEE Trans. on Power Delivery*, vol.1, no.1, pp.1418-1425, 1988.
[28] Y. Mitani, K. Tsuji and Y. Murakami, Application of superconducting magnet energy storage to improve power system dynamic performance, *IEEE Trans. on Power Systems*, vol.3, no.4, pp.143-150, 1986.
[29] L. A. Zadeh, Fuzzy sets, *Information and Control*, vol.8 no.3, pp.338-353, 1965.
[30] E. H. Mamdani, Applications of fuzzy algorithms for simple dynamic plant, *Proc. of IEE*, vol.121, no.12, pp.1585-1588, 1974.
[31] S. Tong, Y. Li and T. Wang, Adaptive fuzzy backstepping fault-tolerant control for uncertain nonlinear systems based on dynamic surface, *International Journal of Innovative Computing, Information and Control*, vol.5, no.10(A), pp.3249-3261, 2009.
[32] L. Luoh, Control design of T-S fuzzy large-scale systems, *International Journal of Innovative Computing, Information and Control*, vol.5, no.9, pp.2869-2880, 2009.
[33] T. Wang, S. Tong and Y. Li, Robust adaptive fuzzy control for nonlinear system with dynamic uncertainties based on backstepping, *International Journal of Innovative Computing, Information and Control*, vol.5, no.9, pp.2675-2688, 2009.
[34] B. M. Mohan and A. Sinha, Analytical structure and stability analysis of a fuzzy PID controller, *Applied Soft Computing*, vol.8, no.1, pp.749-758, 2008.
[35] C. Yang, S. Fan, Z. Wang and W. Li, Application of fuzzy control method in a tunnel lighting system, *Mathematical and Computer Modeling*, vol.54, no.3-4, pp.931-937, 2011.
[36] M. T. Yan and C. C. Fang, Application of genetic algorithm-based fuzzy logic control in wire transport system of wire-EDM machine, *Journal of Materials Processing Technology*, vol.205, no.1-3, pp.128-137, 2008.
[37] J. P. Torreglosa, F. Jurado, P. García and L. M. Fernández, Application of cascade and fuzzy logic based control in a model of a fuel-cell hybrid tramway, *Engineering Applications of Artificial Intelligence*, vol.24, no.1, pp.1-11, 2011.
[38] S. Li, W. Wugao, R. Zhang, D. Lv and Z. Huang, Cascade fuzzy control for gas engine driven heat pump, *Energy Conversion and Management*, vol.46, no.11-12, pp.1757-1766, 2005.

[39] E. Cam, Application of fuzzy logic for load frequency control of hydro-electrical power plants, *Energy Conversion and Management*, vol.48, no.4, pp.1281-1288, 2007.

[40] J. Jamaludin, N. A. Rahim and W. P. Hew, Development of a self-tuning fuzzy logic controller for intelligent control of elevator systems, *Engineering Applications of Artificial Intelligence*, vol.22, no.8, pp.1167-1178, 2009.

[41] C.-B. Chiou, C.-H. Chiou, C.-M. Chu and S.-L. Lin, The application of fuzzy control on energy saving for multi-unit room air-conditioners, *Applied Thermal Engineering*, vol.29, no.2-3, pp.310-316, 2009.

[42] M.-Y. Chen, H.-W. Tzeng, Y.-C. Chen and S.-C. Chen, The application of fuzzy theory for the control of weld line positions in injection-molded part, *ISA Trans.*, vol.47, no.1, pp.119-126, 2008.